Received: 1 October 2025 | Revised: 21 January 2026 | Accepted: 27 February 2026 | Published online: 20 March 2026

RESEARCH ARTICLE

Archives of Advanced Engineering Science
2026, Vol. 4(3) 247–259
DOI: 10.47852/bonviewAAES62027810

BON VIEW PUBLISHING

Analysis of Initial Stress and Linearly Variable Amplitudes of Corrugated Surface on a Fibre-Reinforced Solid Under Magnetic Field and Linearly Varying Impedance

Augustine Igwebuike Anya[1,*] **and Ugochukwu David Uche**[2]

[1] *Department of Mathematical Sciences, Veritas University Abuja, Nigeria*

[2] *Mathematics Programme, National Mathematical Centre Abuja, Nigeria*

Abstract: A mathematical model analyzing the effects of initial stress and variable amplitudes of corrugation for stresses and displacements of surface waves on a fiber-reinforced half-space under a magnetic field and inhomogeneous impedance existing as a linearly varying impedance is proposed. Constitutive equations of homogeneous fiber-reinforced material are utilized in formulating the dynamical equations while incorporating the components of the magnetic field owing to Maxwell's theory of electromagnetism. The normal mode method paved the way in deriving the analytical solution vis-à-vis the stresses and displacements after suitable boundary conditions in terms of linearly varying impedance and linearly varying amplitudes of corrugation (existing as trigonometric Fourier series of diverse heights) were formulated and utilized. Utilizing Mathematica 11, derived stresses and displacements were graphically presented, thus demonstrating the variations of the interacting physical parameters of initial stress, variable amplitudes of corrugation, magnetic fields, and the inhomogeneous impedance. The combined fields' quantities of the model such as the linearly varying impedance and amplitudes of corrugated surface, magnetic field, and initial stress exhibited enormous physical influences on the stresses and displacements of the surface waves on the material. The gradient factor associated with the linearly varying impedance results to a decrease in the behavior of the stresses and displacements on the material when increased. However, an increase in one of the parameters associated with variable amplitudes of corrugation caused an upward trend in the stresses and displacements of the waves. Particular cases are observed from the literatures if we neglect some parameters of variable amplitudes and impedance.

Keywords: varying impedance, linearly varying corrugation, magnetic field, fiber reinforcement, initial stress

1. Introduction

Vibrations are daily phenomena occasioned by natural or artificial occurrences on or in bodies of materials, especially as it behooves on elastic or mechanical waves. These waves on surfaces of materials could be in the forms of Love, Rayleigh, or Stoneley waves, depending on the conditions placed at the boundaries of the interacting interfaces, mathematically speaking, and the economic importance of these waves is predominant to the industries working in the area of geophysics as it concerns seismology, civil and mechanical engineering applications, etc. However, the problem of examining and deciphering information by these vibrations caused in the material bodies requires some models (mathematical models) or experiments via which theories can emanate. More so, it's evident that materials are characterized in different manners or classifications, and it then suffices to say that waves' propagation and modulation would also be entirely in different dimensions. These material classifications could be isotropic or anisotropic based. Spencer [1] formulated his work on the deformation of fiber-reinforced material, which is a particular example of composite materials. Composite materials are anisotropic in nature and have a good level of material quality; thus, this endears them to most engineering applications.

Consequently, studies concerning the surface waves on surfaces of materials using the non-local elasticity theory would still be feasible [2]. This infuses a higher order rate of change to the equations of motion of the wave due to the combined physical consideration of the internal friction and material constants of the medium.

In spite of this, changes in a homogeneous material during deformation result in changes to the state of the medium's characteristics, especially in the material constants. This undoubtedly results in inhomogeneity in the material, be it along the boundary or entirety of the material. Some of these inhomogeneous and non-planar considerations on materials [3, 4] and those reported by Sethi et al. [5] may be in decaying or growing

***Corresponding author:** Augustine Igwebuike Anya, Department of Mathematical Sciences, Veritas University Abuja, Nigeria, Email: anyaa@veritas.edu.ng

© The Author(s) 2026. Published by BON VIEW PUBLISHING PTE. LTD. This is an open access article under the CC BY License (https://creativecommons.org/licenses/by/4.0/).

exponential functions of the material constants in line with the space coordinate of the system via which these surface wave analyses are carried out. Notwithstanding, other forms of inhomogeneity of the material could still occur in the material parameters or the interacting physical factors, but we are laying emphasis to linearly forms of inhomogeneity in materials that include a gradient term. All these linear formulations have ways of giving new meanings and new models to analyze systems of wave phenomena across interfaces and boundaries of materials while retaining the original background of the study for giving negligible factors therein in the formulations.

Furthermore, scientists have always sought ways to incorporate many factors into a model to accurately improve the prediction or decipher information about the system under investigation rather than one known factor, which does not give an accurate account of the environmental, mechanical, or even electrical situation at hand. On this note, Singh [6] employed the mechanical impedance, which is a measure of a material's resistance to wave propagation, while Asano [7] incorporated the corrugated boundary surfaces via trigonometric series representations to make room for the analysis of waves across interfaces or boundaries of materials since some materials are of different geometry (planar and non-planar) or shapes in nature. Thus, delving into models that seek to analyze the displacements and stresses occasioned by waves on the surface of a linearly corrugated and linearly impedance fiber-reinforced medium under initial stress and magnetism highlights the hallmark and objective of this present investigation.

2. Literature Review

Concisely, several researches has been carried out by authors in the literatures by employing other factors like magnetic fields which could alter the material's characteristics and with the propensity to act on the amplitudes and energy ratios and thus affecting wave propagation, initial stress of the material, etc.. This ardently adds to properly study the interactions of waves phenomena and in turn leading to material examination and behavior. Following this, Singh and Tomar [8] as well as Singh et al. [9] provided solutions regarding qP-wave on a corrugated material with two distinct initial stress, examining the influences of corrugation, surface reinforcement, hydrostatic stress, and non-homogeneity on Love waves. Also, simulations of the behavior of steel ferromagnetic fibers commonly used in concrete in a magnetic field were conducted by Nováková et al. [10], while an investigation detailing the application of homogenization approaches to the numerical analysis of seating made of multi-wall corrugated cardboard was conducted by Suarez et al. [11]. Also, studies involving flexural strength of fiber-reinforced concrete as it concerns or relates to the angle of magnetically orientated fibers were proposed by Carrera et al. [12]. Also, other studies such as the analysis of dispersion and damping exhibitions of Love wave on orthotropic visco-elastic Functionally Graded Material (FGM) layer possessing corrugated boundaries were undertaken by Kumari et al. [13] while noting the proposition made by Cáceres-Naranjo et al. [14], which underscores assessment and modeling of corrugated board dynamic properties under impact loads. In line with this, Khalid et al. [15], Kim et al. [16], and Mondal et al. [17] contributed by advancing studies on natural reinforced composites: sustainable materials for emerging applications, dynamic behavior of corrugated cardboard edge damaged by vibration input environments and the mathematical examinations of surface wave transference through imperfect interface in A functionally graded piezoelectric material (FGPM) FGPM-bedded structure as the case may be. The investigation of distinct geometrical aspects of impedance for horizontal impedance conditions was proposed by Maleki and Jafarzadeh [18], while the investigation on the propagation of Stoneley waves for a non-planar interface of double hydrostatic stressed MTI media was brought to light by Chowdhury et al. [19]. More so, studies concerned with Rayleigh waves using impedance boundary conditions and incompressible micropolar and orthotropic material were examined by Singh and Kaur [20, 21]. Similarly, Sahu et al. [22] examined the analysis of Rayleigh waves via mathematical principles for two distinct materials with an imperfect boundary. Giovannini [23] gave account of dipole-exchange spin-wave propagations considering periodically corrugated films, and Rakshit et al. [24, 25] analyzed waves on an imperfect surface of visco-porous piezoelectric half-space under a moving load. Garbowski and Gajewski [26] determined the transverse shear stiffness of sandwich panels with a corrugation using numerical homogenization. Ţălu [27] demonstrated great examination in finding solutions to models involving micro and nanoscale characterization of three-dimensional surfaces. However, all these posited literatures did not account for an investigation on the joint effects of linearly variable amplitudes (i.e., the amplitudes are not constant but change along the surface, thus introducing different layers of complexities to the behavior of the wave) of corrugation and linearly variable impedance (linearly varying impedance infuses non-homogeneity and complex conditions) boundary condition for a homogeneous fiber-reinforced material vis-à-vis analysis of displacements and stresses under magnetic influences. Rather, they treated cases of individual or partial consideration of the interacting physical factors or parameters in order to decipher information about the wave's motion and behaviors on materials.

Owing to the above literatures, the present investigation is conceptualized to account for the mathematical modeling and analysis of surface waves on a variable corrugated and linearly variable impedance medium under the influence of a magnetic field and initial stress. This study is made feasible by utilizing the constitutive stress-strain relations of homogeneous fiber-reinforced solid material with some initial stress incorporations, through which the governing dynamic equations of the wave were developed and presented under the effects of magnetic force. The analytical solution of the model was achieved by adopting the eigenvalue approach of wave analysis. This led to the development and derivation of the components of the displacements and stresses occasioned by the wave motion on the material. Hence, complete or total displacements of the wave and the stresses were achieved by utilizing suitable boundary conditions vis-à-vis linearly variable amplitudes of corrugations and linearly variable impedance of the material. Graphical results for the effects of the combined physical quantities of initial stress, variable amplitudes, variable impedance, and magnetic field parameters on the displacements and stresses of the wave on the material were depicted. We observed that these parameters have great contributions to impact the behaviors of the wave and, by extension, the material through which the waves propagate.

2.1. The mathematical model and formulations

To develop the dynamic equations of the model problem, it is sufficient to clearly state the stress-strain factor of the considered material, the homogeneous fiber-reinforced half-space, as proposed by Spencer [1]. This constitutive relation of a

homogeneous fiber reinforcement has been utilized by Deswal et al. [28] and Anya et al. [3, 29] as follows:

$$\begin{aligned}\tau_{ij} &= \lambda\varepsilon_{kk}\delta_{ij} + 2\mu_T\varepsilon_{ij} + \alpha(q_k q_m \varepsilon_{km}\delta_{ij} + \varepsilon_{kk}q_i q_j)\\ &+2(\mu_L - \mu_T)(q_i q_k \varepsilon_{kj} + q_j q_k \varepsilon_{ki})\\ &+\beta(q_k q_m \varepsilon_{km} q_i q_j) - P\left(\delta_{ij} + \varpi_{ij}\right)\\ &i = j = k = m = 1, 2, 3,\end{aligned} \tag{1}$$

In Equation (1), λ is the Lame's constant, τ_{ij} represents the stress tensor, ε_{ij} gives the strain tensor, u_i entails the displacement vector, P is the initial stress, and δ_{ij} gives the well-known Kronecker delta function and the fiber-reinforced materials (α,β,$(\mu_L - \mu_T)$. The strain tensor is related to the displacement components in the form $\varepsilon_{ij} = \frac{1}{2}\left(u_{i,j} + u_{j,i}\right)$, while the spin tensor is denoted in the form $\varpi_{ij} = \frac{1}{2}\left(u_{i,j} - u_{j,i}\right)$. We represent $\vec{q} = (r_1, r_2, r_3)$ such that $\vec{q} = (1, 0, 0)$ stipulates the fiber-reinforced directions utilized in the model. Thus, utilizing the constitutive relations, the governing or dynamical equation of motion of the wave that inculcates the influence of magnetic force [29] is presented:

$$\tau_{ij,j} + F_i = \rho\ddot{u}_i \tag{2}$$

Where:

$$\begin{aligned}F_i &= \mu_0 H_0^2\ \left(e_{,1} - \varepsilon_0\mu_0\ddot{u}_1, e_{,2} - \varepsilon_0\mu_0\ddot{u}_2, 0\right)\\ &= (F_1, F_2, F_3), i = 1, 2, 3,\end{aligned}$$

$H_i = H_0\delta_{i3} + h_i$, $\mathrm{h_i} = (0\,, 0, -\mathrm{e})$, is induced magnetic field, $\mathrm{e} = \mathrm{u_{i,i}}, \mathrm{i} = \mathrm{i}, 2, \varepsilon_o$ is electric permeability. We propose that the material lies in the plane of x_1x_2 such that $h_i(x_1, x_2, x_3) = -u_{k,k}\delta_{i3}.h_i(x_1, x_2, x_3)\delta_{i3}$. In line with this, we also hold that H_i is the magnetic vector field, and μ_o is the magnetic permeability as accounted by Maxwell's theory. We have equally employed Einstein's summation indices such that the index after the comma entails partial derivatives with respect to the coordinate and the superscript dot gives partial derivatives with respect to time. Owing to all of these submissions and formulations, the dynamical equations of the wave in component forms from Equation (2) are presented:

$$\begin{aligned}&(\lambda + 2\alpha + 4\mu_L - 2\mu_T + \beta + \mu_0 H_0^2)\, u_{1,\,11}\\ &+(\alpha + \lambda + \mu_L + \mu_0 H_0^2 + P/2)\, u_{2,\,21}\\ &+(\mu_L - P/2)u_{1,\,22} = \{\rho + \varepsilon_0\mu_0^2 H_0^2\}\,\ddot{u}_1,\end{aligned} \tag{3}$$

$$\begin{aligned}&(\alpha + \lambda + \mu_L + \mu_0 H_0^2 + P/2)u_{1,\,12} + (\mu_L - P/2)u_{2,\,11}\\ &+(\lambda + 2\mu_T + \mu_0 H_0^2)u_{2,\,22} = \{\rho + \varepsilon_0\mu_0^2 H_0^2\}\ddot{u}_2,\end{aligned} \tag{4}$$

In a compressed form, the coefficients in Equations (3) and (4) can be rewritten as:

$Q_1 = (\lambda + 2\alpha + 4\mu_L - 2\mu_T + \beta + \mu_0 H_0^2)$,
$Q_2 = (\alpha + \lambda + \mu_L + \mu_0 H_0^2)$, $Q_3 = \mu_L - P/2$,
$Q_5 = (\lambda + 2\mu_T + \mu_0 H_0^2)$,
such that:

$$Q_1 u_{1,\,11} + Q_2 u_{2,\,21} + Q_3 u_{1,\,22} = \{\rho + \varepsilon_0\mu_0^2 H_0^2\}\ddot{u}_1, \tag{5}$$

$$Q_2 u_{1,\,12} + Q_3 u_{2,\,11} + Q_5 u_{2,\,22} = \{\rho + \varepsilon_0\mu_0^2 H_0^2\}\ddot{u}_2, \tag{6}$$

As a convenience, if we employ the following dimensionless quantities: $(x_1', x_2', u_1', u_2') = c_0(x_1, x_2, u_1, u_2), c_0^2, = Q_1/\rho$, $(t') = c_0^2\mathrm{t}$, $\tau'_{ij} = \tau_{ij}/\rho c_0^2$ into Equations (5) and (6) and subsequently drop the sign "′" from the achieved equations, we have:

$$u_{1,\,11} + Q_{12}u_{2,\,21} + Q_{13}u_{1,\,22} = \{1 + \varepsilon_0\mu_0^2 H_0^2/\rho\}\ddot{u}_1, \tag{7}$$

$$Q_{12}u_{1,\,12} + Q_{13}u_{2,\,11} + Q_{15}u_{2,\,22} = \{1 + \varepsilon_0\mu_0^2 H_0^2/\rho\}\ddot{u}_2, \tag{8}$$

$$(Q_{12}, Q_{13}, Q_{15}) = ((Q_2, Q_3, Q_5)/Q_1)$$

3. Analytical Solution

In this section, we adopted the principle of the normal mode method, otherwise referred to as the eigenvalue approach, for wave analysis as a strategy and technique employed in formulating our analytical solutions to the stresses and displacements occasioned by the wave on the linearly varying corrugated homogeneous material with linearly varying impedance characteristics under a magnetic field and initial stress on the material. Recall that this approach of analysis is feasible because of the usefulness that resonates with eigenvalue analysis which hinge on a definite fact and as a tool associated with mechanical wave analysis. That is, eigenvalue analysis explored in this work, serves as a means of estimating the vibration shapes and linked frequencies that most structures witness. On applying this proposition, components of the displacements are thus presented:

$$u_i = (\widehat{u}_i(x_2))e^{\omega t + ibx_1}, i = 1, 2. \tag{9}$$

Putting Equation (9) into Equations (7) and (8), two ordinary differential equations (ODEs) are obtained below. These ODEs are made to situate in the direction of the coordinate x_2:

$$(\mathrm{Q_{13}}D^2 - b^2 - K)\widehat{u}_1 + (iQ_{12}bD)\widehat{u}_2 = 0, \tag{10}$$

$$(iQ_{12}bD)\widehat{u}_1 + (\mathrm{Q_{15}}D^2 - Q_{13}b^2 - K)\widehat{u}_2 = 0, \tag{11}$$

$K = (1 + \varepsilon_0\mu_0^2 H_0^2/\rho)\omega^2)$ and D^2 in Equations (10) and (11) entail a second-order ODE in the direction of x_2 of space coordinate. The two equations, namely, Equations (10) and (11), are consequently coupled. This suffices that our 2D analysis seems feasible in the considered direction x_2 and plane of x_1x_2. Thus, by a nontrivial solution, the determinant of Equations (10) and (11) gives zero, whereas $(\widehat{u}_1, \widehat{u}_2)$ is not zero. Thus, via this process, a 4th-order differential equation in D is achieved, or a second-order equation in D^2 is likewise considered and achieved below:

$$(q_{11}(D^2)^2 + q_{12}(D)^2 + q_{13})(\widehat{u}_1, \widehat{u}_2) = 0 \tag{12}$$

The characteristic equation left in D^2 in Equation (12) has complex coefficients $q_{1i}, i = 1, 2, 3$ (Appendix given). These complex coefficients are dependent on the considered material constants. Now, if we assume that η_i, $i = 1, 2$ are real positive roots of Equation (12) and also by utilizing the established propositions of the solution approach, that is, the use of normal mode solution analysis, the solutions of $\widehat{u}_1, \widehat{u}_2$ follow:

$$(\widehat{u}_1, \widehat{u}_2) = (S_n, S_{1n})e^{-\eta_n x_2} n = 1, 2. \tag{13}$$

where the parameters S_n and S_{1n} in Equation (13) are functions of the wavenumber b lying in the direction of x_1 coordinate and ω the

complex frequency. By putting Equation (13) into Equations (10) and (11), the established relation for S_{1n}, which is in terms of S_n, is presented:

$$\begin{aligned} S_{1n} &= N_{1n}S_n, \\ N_{1n} &= h_{1n}/h_{2n}, \\ h_{1n} &= (\mathrm{Q}_{13}\eta_n^2 - b^2 - K + (iQ_{12}b\eta_n), \\ h_{2n} &= (\mathrm{Q}_{15}\eta_n^2 - Q_{13}b^2 - K + (iQ_{12}b\eta_n). n = 1, 2. \end{aligned} \tag{14}$$

Subsequently, the total components of horizontal and normal displacements and normal and tangential stresses produced by the surface wave on the fiber-reinforced solid under magnetic field and initial stress become:

$$\begin{aligned} u_1 &= S_n e^{-\eta_n x_2 + \omega t + ibx_1}, \\ u_2 &= S_n N_{1n} e^{-\eta_n x_2 + \omega t + ibx_1}, \\ \tau_{11} &= \{ib(1 - (\mu_0 H_0^2/Q_1)) - \eta_n N_{1n} Q_{16}\} S_n e^{-\eta_n x_2 + \omega t + ibx_1} \\ &\quad -P/\mathrm{Q}_1, \\ \tau_{22} &= \{ibQ_{16} - \eta_n N_{1n} Q_{17}\} S_n e^{-\eta_n x_2 + \omega t + ibx_1} - P/\mathrm{Q}_1, \\ \tau_{12} &= \{ibN_{1n} Q_{31} - \eta_n Q_{13}\} S_n e^{-\eta_n x_2 + \omega t + ibx_1}, \\ \tau_{21} &= \{ibN_{1n} Q_{13} - \eta_n Q_{31}\} S_n e^{-\eta_n x_2 + \omega t + ibx_1}, \; n = 1, 2. \\ Q_{16} &= (\lambda + \alpha)/\mathrm{Q}_1, \mathrm{Q}_{17} = (\lambda + 2\mu_T)/\mathrm{Q}_1, \mathrm{Q}_{31} \\ &= (\mu_L + P/2)/\mathrm{Q}_1. \end{aligned}$$

4. Linearly Varying Impedance and Linearly Variable Amplitudes of Corrugated Surface

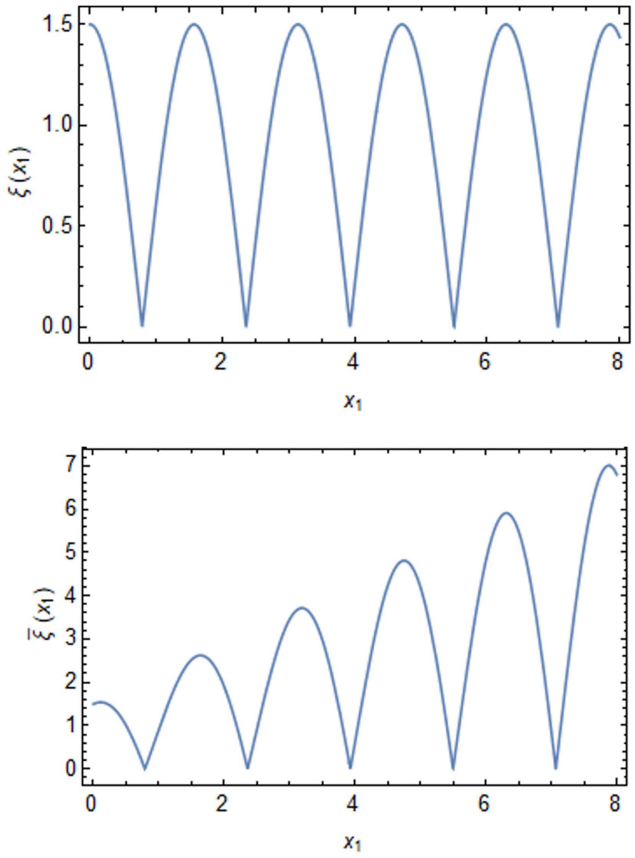
In this section, we devote the formulations to introduce the linearly varying impedance and linearly varying corrugation that define our new model under investigation. From the background of previous investigation, Asano [7] had proposed $\xi(x_1) = \xi_l e^{ilbx_1} + \xi_{-l} e^{-ilbx_1}, l = 1, 2, 3, 4, ...$for all $x_2 = \xi(x_1)$ at the boundary. Now, $x_2 = \xi(x_1)$ defines the corrugation but with no variation in the amplitude. This is because Asano [7] considered $x_2 = \xi(x_1) = a\cos bx_1$. Here, ξ_l and ξ_{-l} entail the Fourier expansion coefficients, and l is the series expansion order, a the uniform amplitude of corrugation, and b the wavenumber. However, we need to include a variation in the corrugation such that $x_2 = \xi(x_1) = a\cos bx_1$ is reformulated. In doing so, we introduce $\bar{\xi}(x_1) = \bar{\xi}_l e^{ilbx_1} + \bar{\xi}_{-l} e^{-ilbx_1}, l = 1, 2, 3, 4, ...$ such that $\bar{\xi}(x_1) = \bar{\xi}_l e^{ilbx_1} + \bar{\xi}_{-l} e^{-ilbx_1}, l = 1, 2, 3, 4, ..., \bar{\xi}_1^{\pm} = (a + cx_1)/2$, and $\bar{\xi}_l^{\pm} = (F_l + I_l)/2, \; l = 2, 3...$On expansion into trigonometry series, this implies that

$$\begin{aligned} \bar{\xi}(x_1) = (a + cx_1)\cos bx_1 + F_2 \cos 2bx_1 + \\ I_2 \sin 2bx_1 + ... + F_l \cos lbx_1 + I_l \sin lbx_1. \end{aligned}$$

Hence, following Asano [7] and our formulation in this regard, it suffices to state that $\bar{\xi}(x_1) = (a + cx_1)\cos bx_1$, where $(a + cx_1)$ gives the variable amplitudes linked with the corrugated surface. Thus, it implies that our new model shall adopt the variable amplitudes of corrugation $\bar{\xi}(x_1) = (a + cx_1)\cos bx_1$ and when $c = 0$, $\bar{\xi}(x_1) = (a + cx_1)\cos bx_1$ returns to $\xi(x_1) = a\cos bx_1$ [7]. To demonstrate the two different corrugations in Figure 1, we have plotted $\xi(x_1) = a\cos bx_1$ and $\bar{\xi}(x_1) = (a + cx_1)\cos bx_1$ as (a) and (b), respectively, below:

Following the above submissions, the boundary conditions associated with the material with linearly variable amplitudes of

Figure 1
(a) Constant amplitude of corrugation Asano and (b) linearly variable amplitudes of corrugation



corrugation and linearly varying impedance for an initially stressed homogeneous solid become:

1) Normal stress w.r.t $x_2 = \bar{\xi}(x_1)$ entails the condition: $\tau_{22} + \bar{\tau}_{22} - \overline{\xi'}(x_1)\sigma_{21} + \omega\widehat{Z}_2 u_2 + P = 0, \forall x_1$ and t. Where $\bar{\tau}_{22} = \mu_0 H_0^2(u_{1,1} + u_{2,2})$, Spencer [1] define a new stress on the material as proposed by Maxwell's theory.
2) The tangential stress stipulates: $\tau_{12} - \overline{\xi'}(x_1)\tau_{11} + \omega\widehat{Z}_1 u_1 + P\varpi_{12} = 0, x_2 = \bar{\xi}(x_1)\forall x_1$ and t, [1, 28]. $\widehat{Z}_1$ and $\widehat{Z}_2$ [29, 30] give the parameters of inhomogeneity of the impedance of the material. Our study justifies the fact that $\widehat{Z}_1, \widehat{Z}_2$ would denote and connote a linearly varying impedance such that $(\widehat{Z}_1, \widehat{Z}_2) = (Z_1, Z_2)(1 + dx_2)$. However, Z_1, Z_2 are considered homogeneous if d, which is the gradient factor of the linearly varying impedance, is zero, meaning that we are sure that we can retrieve Z_1, and Z_2 given $d = 0$. Following this, it entails that these assumptions give the two systems of nonhomogeneous algebraic equations of linearly varying impedance boundary condition of a homogeneous variable corrugated half-space given below:

$$\begin{aligned} &\{ibQ_{16} - \eta_n N_{1n} Q_{17}\} e^{-(\eta_n)\xi(x_1)} S_n \\ &+ [(a + cx_1)b\sin bx_1 - c\cos bx_1] \\ &\quad \{(ibN_{1n} - \eta_n)Q_{13}\} e^{-(\eta_n)\xi(x_1)} S_n \\ &+ \{\mu_0 H_0^2(ib - \eta_n N_{1n}\} e^{-(\eta_n)\xi(x_1)} S_n \\ &+ \omega N_{1n} Z_2(1 + d\xi(x_1)) e^{-(\eta_n)\xi(x_1)} S_n = 0, \end{aligned} \tag{15}$$

$$
\begin{aligned}
&\{\{ibN_{1n}-\eta_n\}Q^*_{13}S_n+[(a+cx_1)b\sin bx_1\\
&\quad -c\cos bx_1]\{ib(1-(\mu_0H_0^2/\mathrm{Q}_1))\\
&\quad -\eta_nN_{1n}Q_{16}\}S_n\}e^{-(\eta_n)\xi(x_1)}\\
&\quad +\omega Z_1(1+d\xi(x_1))S_ne^{-(\eta_n)\xi(x_1)}\\
&\quad =P/\mathrm{Q}_1[(a+cx_1)b\sin bx_1-c\cos bx_1],\\
&\quad n=1,2.
\end{aligned}
\tag{16}
$$

Here, $Q^*_{13}=\mu_L/\mathrm{Q}_1$ and finding solutions of the algebraic system of 2×2 equations (Equations (15) and (16)) for S_n, $n=1,2$ aid our derivations of the analytical results vis-à-vis the displacements and stresses of the surface waves on the linearly varying impedance-corrugated homogeneous magneto-elastic material. We equally observed that if the variable amplitude parameter $c=0$, this yields results for Asano's [7] model for constant amplitudes of corrugated surface of the material, while $d=0$ would generate results for uniform or constant impedance considerations found in the literatures.

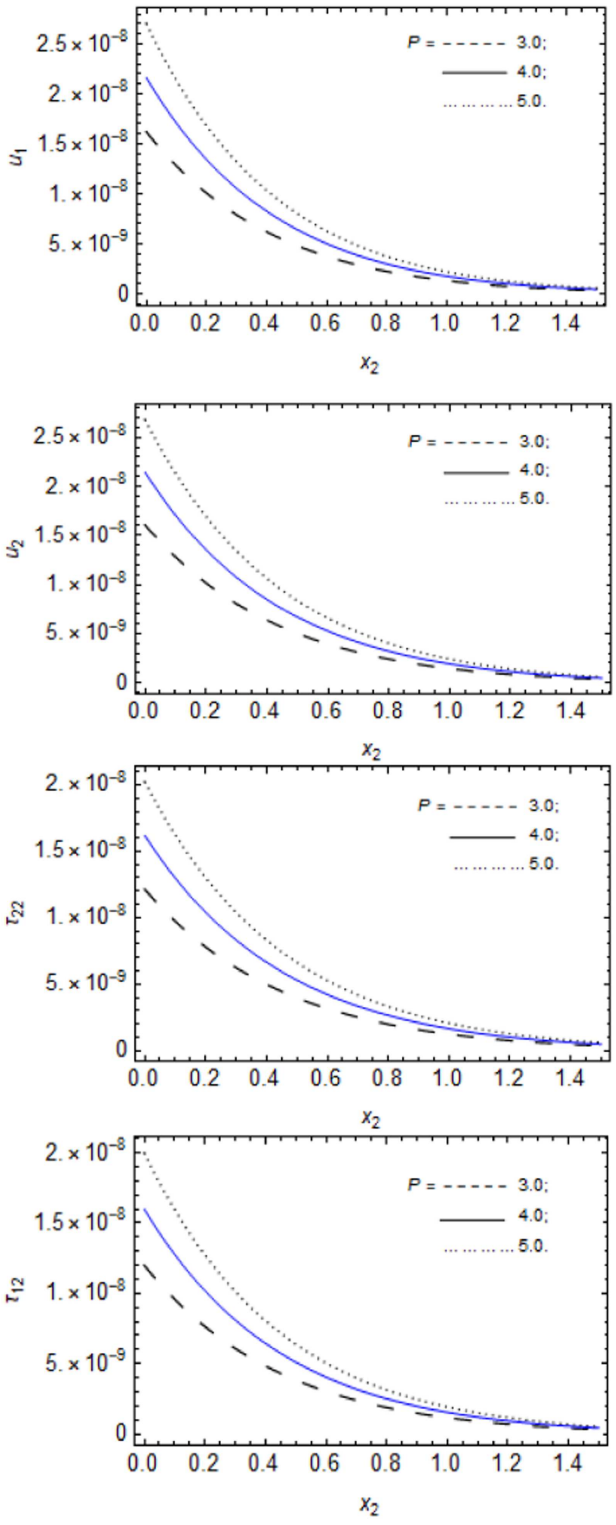
5. Computational Results and Discussion

The analytical solutions of the displacements and stresses of the surface wave on the material are depicted in graphical forms and are equally discussed in this section by utilizing the computational tool Mathematica. This is in order to draw conclusions from the behaviors of the combined interactions occasioned by the initial stress parameter, variable amplitude parameters(a,c), magnetic field H_0, impedance $Z_i, i=1,2$, and the gradient factor d associated with the varying impedance on the displacements and stresses of the complex geometry. Utilizing the numerical parameters [31] and other quantities as given below, the graphics and their corresponding analysis are thus presented in Figures 2–9.

$$
\begin{aligned}
&\lambda=3.76\times10^9 kg\,m^{-1}s^{-2};\mu_L=7.86\times10^9 kg\,m^{-1}s^{-2};\\
&\mu_T=2.86\times10^9 kg\,m^{-1}s^{-2};\rho=7800 kg\,m^{-3};\\
&\alpha=-1.78\times10^9 kg\,m^{-1}s^{-2};\ \beta=2\times10^9 kg\,m^{-1}s^{-2};\\
&\omega=(0.8-0.5i)rad/s;t=0.2s;b=0.3m^{-1};\\
&Z_1=0.05;Z_2=0.07;c=0.7;a=0.25m,\\
&H_0=1000A/m;d=0.5m;P=3N/m^2
\end{aligned}
$$

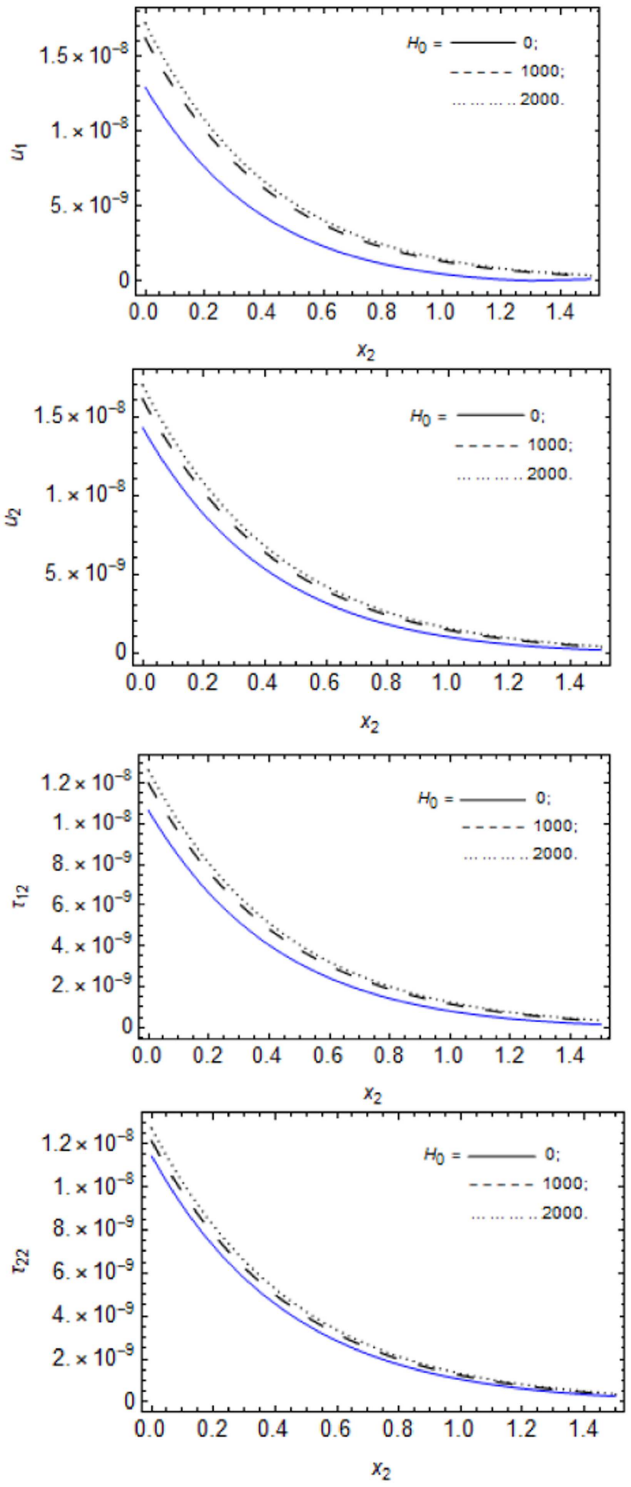
In Figure 2, we depict the impact of the initial stress P on the displacements $u_i, i=1,2$ and stresses (τ_{12} and τ_{22}) of the waves on the material versus the length x_2 of the material. This happens when the interacting physical parameters of variable amplitude parameters (a,c), magnetic field H_0, impedance $Z_i, i=1,2$, and the gradient factor d associated with the linear varying impedance are unchanged on the material for varying initial stress P. Sequel to this, we witness that the initial stress on the material caused increase in behaviors on the displacements and stresses of the wave on the material when increased. Also, this increase is observed to be in sequence starting from the initial length of the material, where their maximum values occur. On this note, as the wave propagates along the extended length of the material, decrease effects in terms of amplitudes and behaviors of the displacements and stresses were observed and via which the minimum decrease effects values lie especially at the vanishing region of the waves; $P=3$. Physically speaking, the initial stress P has shown that its impact for this considered model is to act as a push on the material, thus increasing the displacements and stresses occasioned by the surface wave on the corrugated surface.

Figure 2
Effects of initial stress (N/m^2) on the displacements in meters and stresses (and) in (N/m^2) with respect to in meters



Accordingly, Figure 3 demonstrates the influence of the magnetic field H_0 on the displacements $u_i, i=1,2$ and stresses (τ_{12}andτ_{22}) of the waves on the material against the length x_2 of the material. This occurrence is feasible only when the combined interacting physical parameters of variable amplitude parameters (a,c), initial stress P, wavenumber b, impedance $Z_i, i=1,2$, and

Figure 3
Effects of magnetic field H_0 (A/m) on the displacements $u_i, i = 1, 2$ in meters and stresses (τ_{12} and τ_{22}) in (N/m^2) with respect to x_2 in meters



the gradient factor d associated with the linear varying impedance are unchanged in the material for the different magnetic field H_0. Owing to this, we observed that the magnetic field H_0 on the material caused an increase in behaviors on the displacements and stresses of the wave on the material when increased, however, not in a sequential manner. The maxima displacements and stresses of the wave lie near $x_2 = 0$. Decrease across the material as the wave propagates along the extended length of the material in terms of amplitudes and behaviors of the displacements and stresses were recorded and towards this region, the minimum values lies across the material as especially at the vanishing region of the waves; $H_0 = 0$-given that the magnetic field is negligible.

Nevertheless, Figure 4 gives the pictorial evidence demonstrated by the gradient factor d associated with the linearly varying impedance (linear inhomogeneous impedance) on the displacements $u_i, i = 1, 2$ and stresses (τ_{12} and τ_{22}) of the surface waves on the material with respect to $x_2$coordinate of space. This is such that the other physical constants of magnetic field H_0, variable amplitude parameters(a, c), wavenumber b, initial stress P, and impedance $Z_i, i = 1, 2$ are held fixed on the material. More so, we notice that from Figure 4, increasing the gradient factor $d$associated with the linearly varying impedance (linear inhomogeneous impedance) results to a decrease in the behavior of the stresses and displacements of the surface waves on the material. Hence, we equally observed that the maximum values of the stresses and displacements occur near the origin of the normal coordinate of space x_2, while their minimum values lie at the point or region of vanishing point of the wave on the material where uniform behaviors occur. This physically has some level of conviction patterning to how the nature of impedance could influence wave propagation.

Subsequently, Figure 5 showcases the effects of the parameter a associated with variable amplitudes of corrugated surface on the displacements $u_i, i = 1, 2$ and stresses (τ_{12} and τ_{22}) of the surface waves on the material with respect to the normal coordinate x_2 such that the wavenumber b, magnetic field H_0, variable amplitude parameter$c$, initial stress P, the gradient factor d associated with the linearly varying impedance (linear inhomogeneous impedance), and impedance $Z_i, i = 1, 2$ were steady on the solid half-space. In addition, we witness from the profiles in Figure 5 that an increase in the parameter a associated with variable amplitudes of corrugation gives a corresponding increase in the stresses and displacements of the waves on the material. This increase entails that at $a = 2.70$, we have more amplitude and behavior of the stresses and displacements of the wave on the material, especially close to the origin of the normal coordinate, that is, at $x_2 = 0$. It is also observed that this increase was evenly, sequentially, and upwardly distributed. However, the minimum values were attained toward the vanishing region and the end part of the material along the normal coordinate at this instance.

Sequel to this, Figure 6 depicts the impacts of wavenumber b associated with the corrugated surface on the displacements $u_i, i = 1, 2$ and stresses (τ_{12} and τ_{22}) of the surface waves on the material with respect to the normal coordinate x_2. This impact will only become feasible in considerations where the magnetic field H_0, variable amplitudes parameter (c, a), initial stress P, the gradient factor d associated with the linearly varying impedance (linear inhomogeneous impedance), and impedance $Z_i, i = 1, 2$ were unchanged on the fiber-reinforced half-space. In line with this, observations were made from the profiles in Figure 6 such that an increase in the wavenumber gives a decrease in the stresses and displacements of the waves on the solid. This decrease entails that at $b = 0.8$, we have downward trends on the amplitudes and behavior of the stresses and displacements of the wave on the material, thus yielding minimum values. We observed that the maximum values of the distributions of the displacements and stresses occur near the origin of the normal coordinate, that is, at $x_2 = 0$. Hence, it suffices that as the wave propagates on the material from the origin and then across the material, decrease effects

Figure 4
Effects of the gradient factor d associated with the linearly varying impedance (inhomogeneous impedance) on the displacements $u_i, i = 1, 2$ in meters and stresses (τ_{12} and τ_{22}) in (N/m^2) with respect to x_2 in meters

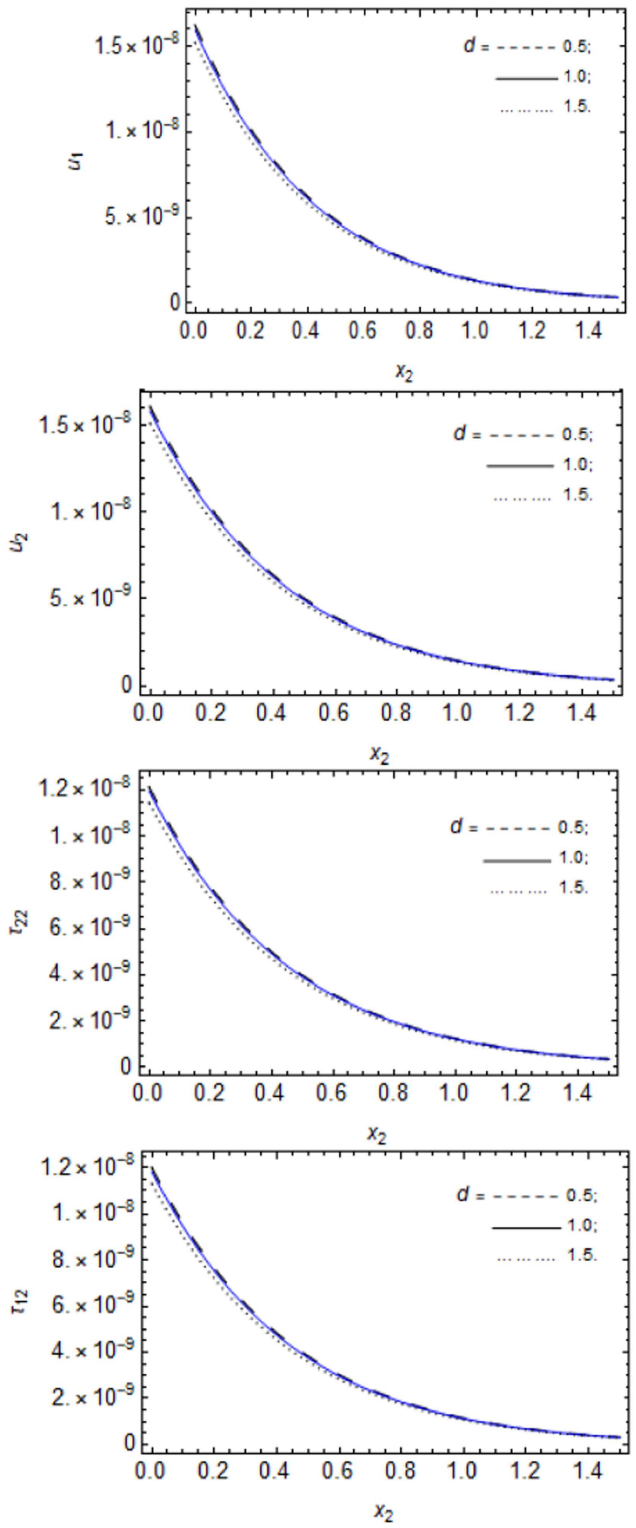


Figure 5
Effects of a(m) associated with variable amplitudes of corrugation on the displacements $u_i, i = 1, 2$ in meters and stresses (τ_{12} and τ_{22}) in (N/m^2) with respect to x_2 in meters

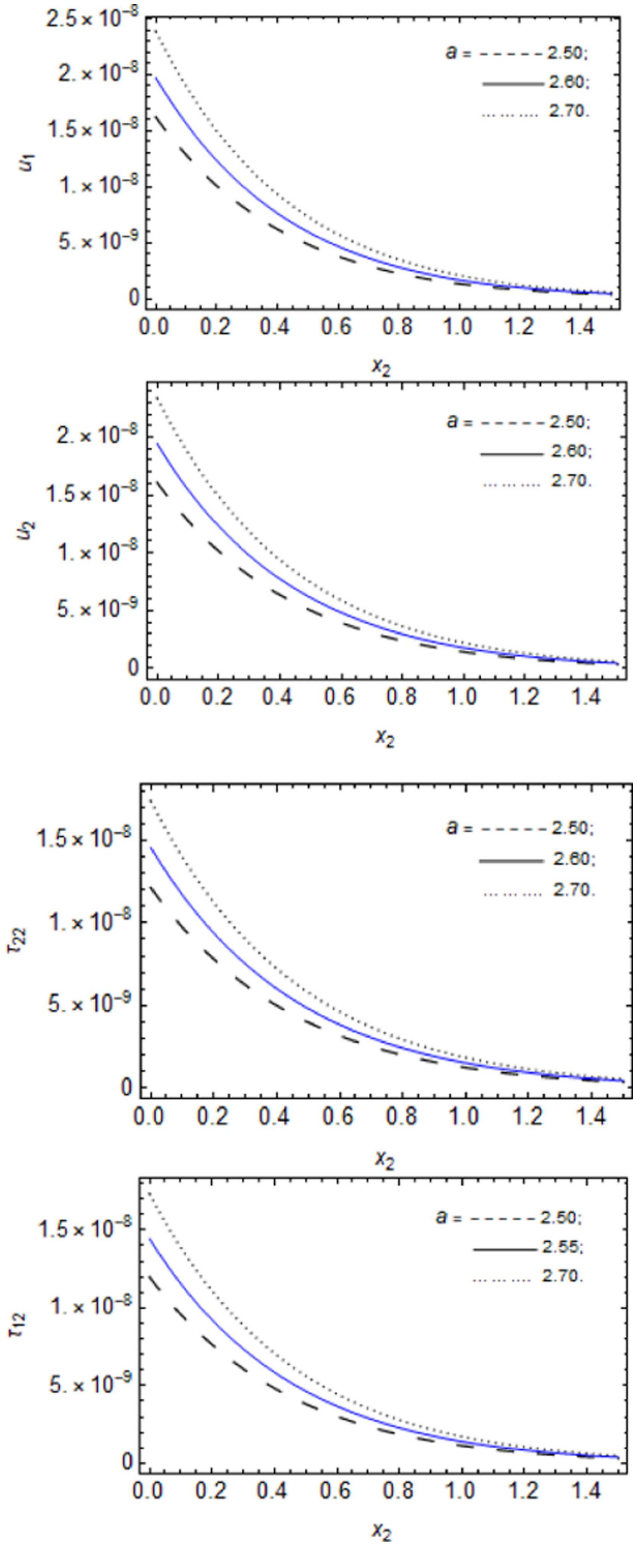
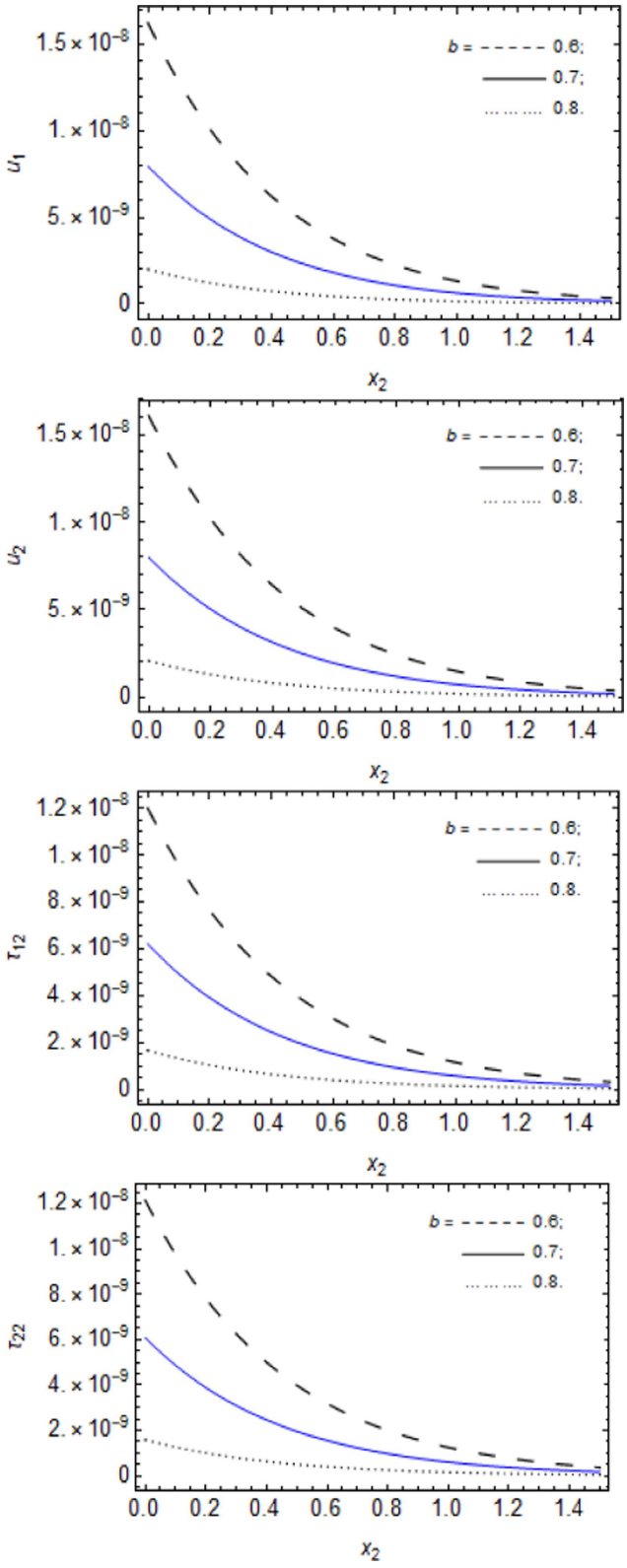


Figure 6
Effects of wavenumber b (m^{-1}) on the displacements $u_i, i = 1, 2$ in meters and stresses (τ_{12} and τ_{22}) in (N/m^2) with respect to x_2 in meters



are felt. Hence, more wavenumber on the material would trigger reduced displacements and stresses of the wave on the linearly corrugated and linear impedance surface.

Figure 7 also demonstrates the influence of c associated with variable amplitude of corrugation on the displacements $u_i, i = 1, 2$ and stresses (τ_{12} and τ_{22}) of the surface waves on the material with respect to the normal coordinate x_2.This ensues if the contributing quantities of wavenumber b, magnetic field H_0, variable amplitude parameter (a), initial stress P, the gradient factor d associated with the linearly varying impedance (linear inhomogeneous impedance), and impedance $Z_i, i = 1, 2$ were in constant application on the fiber-reinforced half-space. Following this, observations were made from the profiles in Figure 7 such that an increase in the c associated with variable amplitude of corrugation produces a corresponding increase or upward trends in the stresses and displacements of the waves on the solid. This increase entails that at $c = 0.9$, we have upward trends on the amplitudes and behavior of the stresses and displacements of the wave on the material, thus yielding maximum values. Hence, as the wave propagates on the material from the origin and then across the length of the material, decrease effects are witnessed owing to the material compositions. More so, the minimum values of the displacements and stresses of the material were attained when $c = 0.6$.

Furthermore, Figure 8 stipulates the influence of the normal impedance Z_2 on the displacements $u_i, i = 1, 2$ and stresses (τ_{12} and τ_{22}) of the surface waves on the material with respect to the normal coordinate x_2. These effects take place if the combined quantities of wavenumber b, magnetic field H_0, variable amplitudes parameter (a, c), initial stress P, the gradient factor d associated with the linearly varying impedance (linear inhomogeneous impedance), and impedance Z_1 were held fixed on the fiber-reinforced medium. Consequently, we observe that the profiles in Figure 8, that is, the displacements and stresses of the waves on the material, slightly decrease for an increase in the normal impedance Z_2 on the material. However, uniform characteristics are felt toward the extended part of the length of the material where the minimum values lie. This region of uniform behavior attests to the negligibility of the variations of the impedance Z_2 on the distributions. While the maximum values of the distributions lie near the origin, that is, at $x_2 = 0$, we can deduce that the physical implication of impedance is being felt by the wave on the material such that a resistant-like phenomenon that drags the motion of the wave from experiencing adequate change is noticed.

However, Figure 9 demonstrates the impacts of the horizontal impedance Z_1on the displacements $u_i, i = 1, 2$ and stresses (τ_{12} and τ_{22}) of the surface waves on the material with respect to the normal coordinatex_2. This occurrence would be feasible if the wavenumber b, magnetic field H_0, variable amplitudes parameter (a, c), initial stress P, the gradient factor d associated with the linearly varying impedance (linear inhomogeneous impedance), and impedance Z_2 were applied constantly on the material. Following this, we observe that the distributions in Figure 9, that is, the displacements and stresses of the waves on the material, slightly show uniform behavior for an increase in the horizontal impedance Z_1 on the material. However, complete uniform behaviors are witnessed toward the extended part of the length of the material where the minimum values lie. This portion of uniform behavior on the material attests to the negligibility of the variations of the impedance Z_1on the distributions. That is, for $x_2 \geq 0.5$, uniform behaviors occur. The maximum values of the distributions are attained near the origin, that is, at $x_2 = 0$. We can infer that the physical consequences of the impedance are being felt by the wave on the material, such that drags on the motion of the wave may become evident.

Figure 7
Effects of $c(m)$ associated with variable amplitude of corrugation on the displacements $u_i, i = 1, 2$ in meters and stresses (τ_{12} and τ_{22}) in (N/m^2) with respect to x_2 in meters

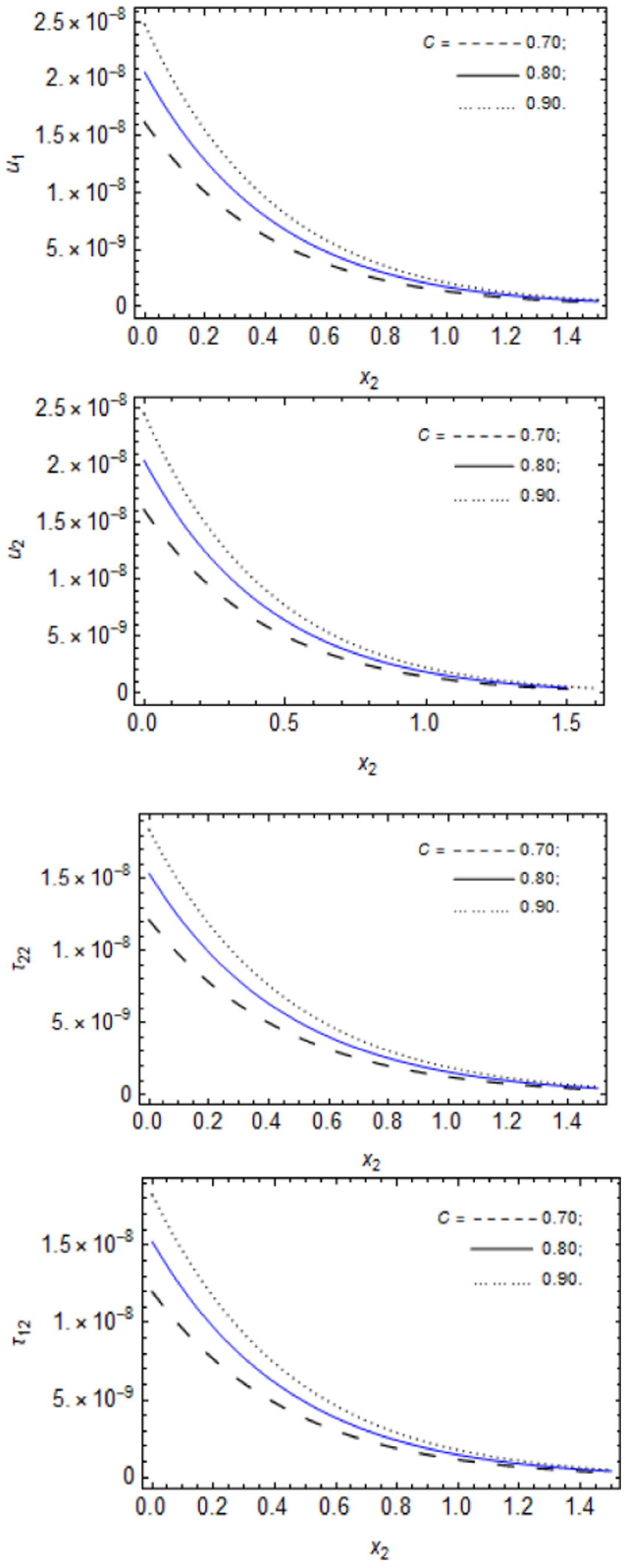


Figure 8
Effects of impedance Z_2 on the displacements $u_i, i = 1, 2$ in meters and stresses (τ_{12} and τ_{22}) in (N/m^2) with respect to x_2 in meters

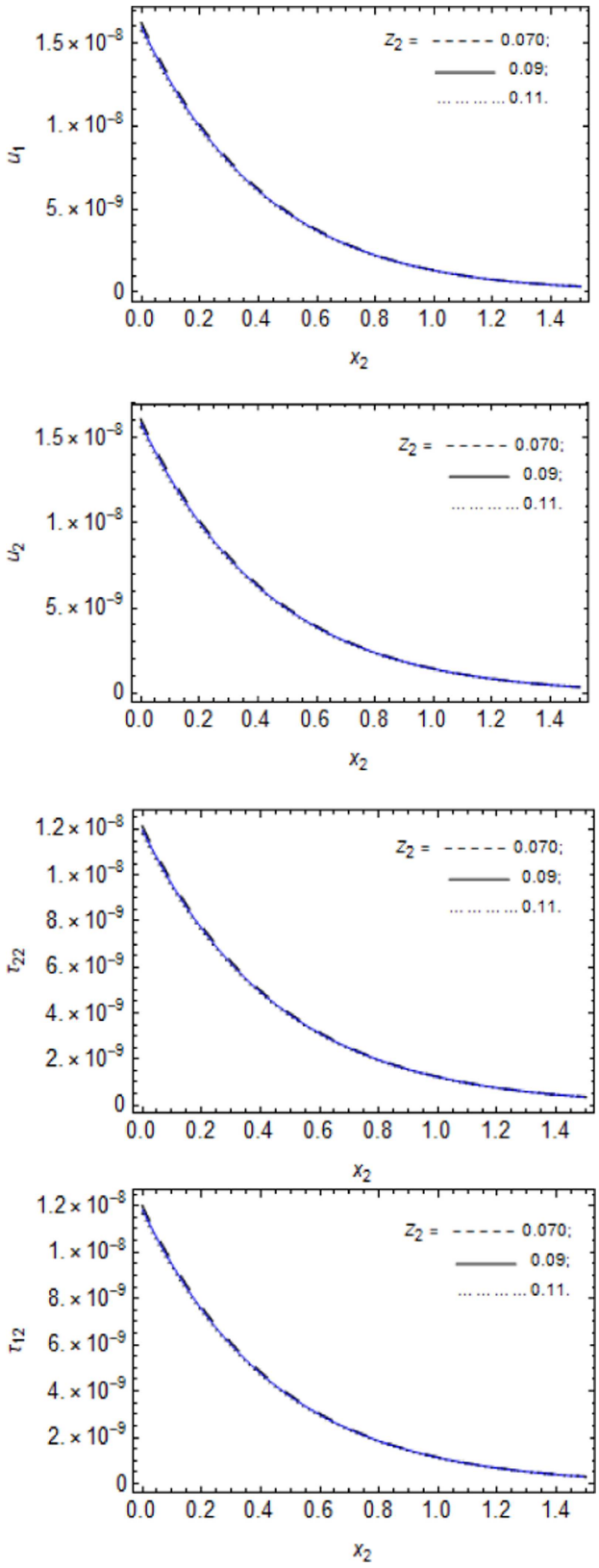
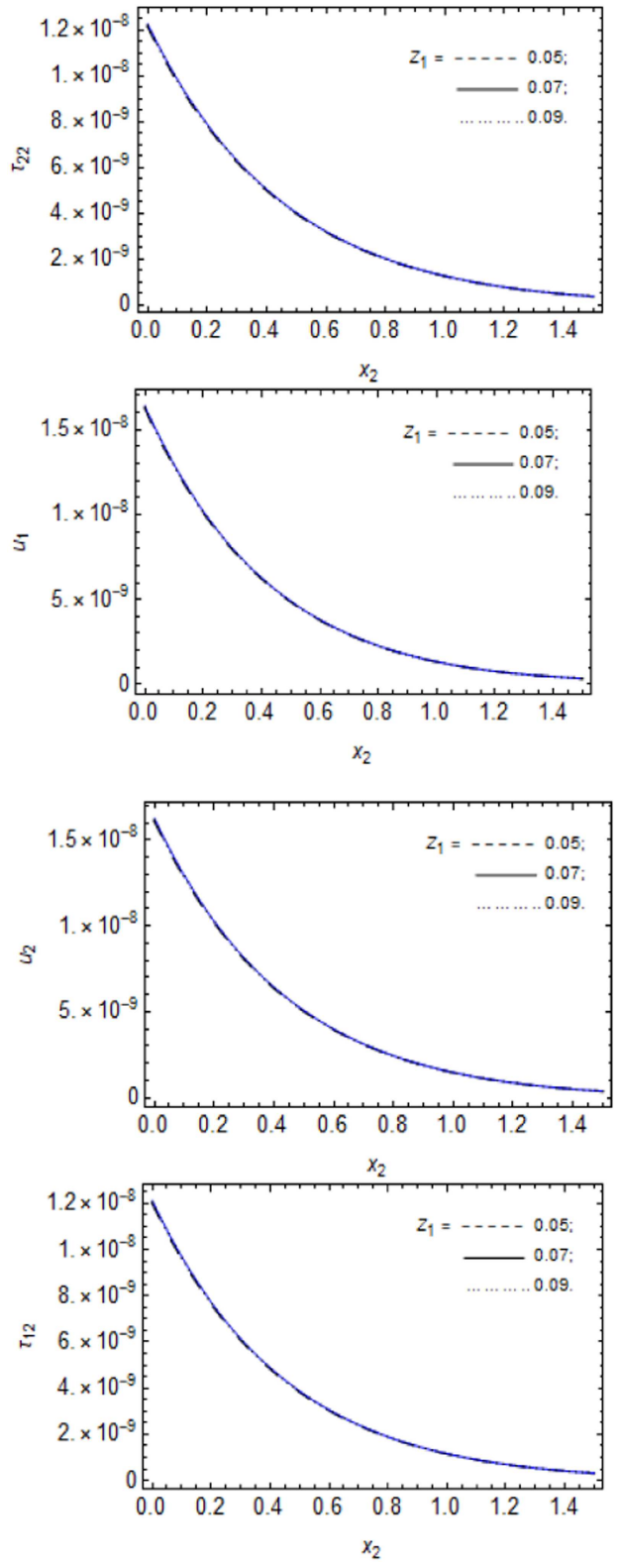


Figure 9
Effects of impedance Z_1 on the displacements $u_i, i = 1, 2$ in meters and stresses (τ_{12} and τ_{22}) in (N/m^2) with respect to x_2 in meters



6. Conclusion

This study developed and explored the fundamental 2D model analysis for the impacts of initial stress, linearly variable impedance, and linearly variable amplitudes of corrugated boundary conditions on the displacements and stresses of surface waves on a homogeneous fiber-reinforced solid with the influences of a magnetic field. The equations of motion of the surface wave were derived by the use of the fiber-reinforced stress-strain relation along with the interacting magnetic field. Through the formulations of suitable boundary conditions of linearly variable impedance and linearly variable amplitudes of corrugations of the medium, the analytical solutions of the displacements and stresses of the wave were derived after utilizing the harmonic solution method. Combined impacts of the interacting quantities of the model such as the magnetic field, linearly varying impedance, linearly variable amplitudes of corrugation parameters, wavenumber, and initial stress on the displacements and stresses of the surface waves were ascertained through depiction of the analytical solutions in graphical forms with their corresponding analysis. Following this, we observe that:

1) Increase in the initial stress, parameter a associated with variable amplitudes of corrugated surface, and magnetic field yields a corresponding increase in behavior on the displacements and stresses of the surface wave on the fiber-reinforced medium.
2) The gradient factor d associated with the linearly varying impedance (linear inhomogeneous impedance) results to a decrease in the behavior of the stresses and displacements of the surface waves on the material when increased.
3) The displacements and stresses of the waves on the material slightly decrease for an increase in the normal impedance Z_2 on the material. However, uniform characteristics are also felt toward the extended part of the length of the material, while an increase in the horizontal impedance Z_1 slightly shows uniform behavior on the distribution of the stresses and displacements. We can deduce that the physical implications of the impedance are being felt by the wave on the material, such that drags on the motion of the wave may become evident.
4) The wavenumber stipulates a decrease in the stresses and displacements of the waves on the solid when in an upward trend.

Increase in the parameter c associated with variable amplitude of corrugation produces an upward trend in the stresses and displacements of the waves.

In a nutshell, our results in this study show that specific results in the literatures would be obtainable if we consider the gradient factor $d$associated with the linearly varying impedance to be zero, thereby leading to a homogeneous impedance model. Also, if we neglect the parameter$a$associated with variable amplitudes of corrugated surface, the result for Asano [7] for constant amplitude of corrugated surface is achieved. On this note, the study would prove to be useful and applicable to works that encompass wave phenomena and material designs. Engineering applications that involve destructive testing and actuator device mechanisms are prominent areas of interest where this work would prove useful.

Nomenclatures

d = Parameter associated with the linearly varying impedance
H_0 = Magnetic field
b = Wavenumber
a, c = Parameters associated with variable amplitude of corrugation
τ_{ij} = Stress tensor
ε_{ij} = Strain tensor

u_i = Displacement vector
δ_{ij} = Kronecker delta function
λ = Lame's constant
$(\alpha,\beta,(\mu_L - \mu_T))$ = Fiber-reinforced parameters
ρ = Density
x_i = Coordinates
Z_1, Z_2 = Impedance parameters

Ethical Statement

This study does not contain any studies with human or animal subjects performed by any of the authors.

Conflicts of Interest

The authors declare that they have no conflicts of interest to this work.

Data Availability Statement

The data for fiber-reinforced material in this study is taken from published work of Othman et al. [31]. Data is available in the Computational Results and Discussion section.

Author Contribution Statement

Augustine Igwebuike Anya: Conceptualization, Methodology, Software, Validation, Formal analysis, Investigation, Resources, Data curation, Writing – original draft, Writing – review & editing, Visualization, Supervision, Project administration. **Ugochukwu David Uche:** Methodology, Software, Validation, Data curation, Writing – review & editing, Visualization, Supervision, Project administration.

References

[1] Spencer, A. J. M. (1972). *Deformations of fibre-reinforced materials*. UK: Oxford University Press.

[2] Barak, M. S., & Dhankhar, P. (2023). Thermo-mechanical interactions in a rotating nonlocal functionally graded transversely isotropic elastic half-space. *Journal of Applied Mathematics and Mechanics*, *103*(2), e202200319. https://doi.org/10.1002/zamm.202200319

[3] Anya, A. I., Uche, U. D., & Nwachioma, C. (2025). Mathematical analysis on dispersion relation of Rayleigh wave for an initially stressed magneto-poroelastic material with corrugated and impedance boundary. *Archives of Advanced Engineering Science*, *3*(3), 163–170. https://doi.org/10.47852/bonviewAAES42021903

[4] Barak, M. S., Poonia, R., Devi, S., & Dhankhar, P. (2024). Nonlocal and dual-phase-lag effects in a transversely isotropic exponentially graded thermoelastic medium with voids. *Journal of Applied Mathematics and Mechanics*, *104*(5), e202300579. https://doi.org/10.1002/zamm.202300579

[5] Sethi, M., Sharma, A., & Sharma, A. (2016). Propagation of SH waves in a double non-homogeneous crustal layers of finite depth lying over an homogeneous half-space. *Latin American Journal of Solids and Structures*, *13*(14), 2628–2642.

[6] Singh, B. (2017). Reflection of elastic waves from plane surface of a half-space with impedance boundary conditions. *Geosciences Research*, *2*(4), 242–253. https://doi.org/10.22606/gr.2017.24004

[7] Asano, S. (1966). Reflection and refraction of elastic waves at a corrugated interface. *Bulletin of the Seismological Society of America*, *56*(1), 201–221. https://doi.org/10.1785/BSSA0560010201

[8] Singh, S. S., & Tomar, S. K. (2008). *qP*-wave at a corrugated interface between two dissimilar pre-stressed elastic half-spaces. *Journal of Sound and Vibration*, *317*(3-5), 687–708. https://doi.org/10.1016/j.jsv.2008.03.036

[9] Singh, A. K., Das, A., Kumar, S., & Chattopadhyay, A. (2015). Influence of corrugated boundary surfaces, reinforcement, hydrostatic stress, heterogeneity and anisotropy on Love-type wave propagation. *Meccanica*, *50*(12), 2977–2994. https://doi.org/10.1007/s11012-015-0172-6

[10] Nováková, K., Carrera, K., Konrád, P., Künzel, K., Papež, V., & Sovják, R. (2022). Simulations of the behaviour of steel ferromagnetic fibres commonly used in concrete in a magnetic field. *Materials*, *15*(1), 128. https://doi.org/10.3390/ma15010128

[11] Suarez, B., Muneta, M. L. M., Sanz-Bobi, J. D., & Romero, G. (2021). Application of homogenization approaches to the numerical analysis of seating made of multi-wall corrugated cardboard. *Composite Structures*, *262*, 113642. https://doi.org/10.1016/j.compstruct.2021.113642

[12] Carrera, K., Künzel, K., Papež, V., Sovják, R., Kheml, P., Fornůsek, J., . . . , & Konrád, P. (2022). Flexural strength of fibre reinforced concrete in relation to the angle of magnetically orientated fibres. *MATEC Web of Conferences*, *364*, 05017. https://doi.org/10.1051/matecconf/202236405017

[13] Kumari, C., Kundu, S., Kumari, A., & Gupta, S. (2020). Analysis of dispersion and damping characteristics of Love wave propagation in orthotropic visco-elastic FGM layer with corrugated boundaries. *International Journal of Geomechanics*, *20*(2), 04019172. https://doi.org/10.1061/(ASCE)GM.1943-5622.0001569

[14] Cáceres-Naranjo, D., Bernad, C., Calvo, S., & Royo, J. M. (2023). Assessment and modelling of corrugated board dynamic properties under impact loads. Application to edge crush disposition. *Results in Engineering*, *18*, 101072. https://doi.org/10.1016/j.rineng.2023.101072

[15] Khalid, M. Y., Al Rashid, A., Arif, Z. U., Ahmed, W., Arshad, H., & Zaidi, A. A. (2021). Natural fiber reinforced composites: Sustainable materials for emerging applications. *Results in Engineering*, *11*, 100263. https://doi.org/10.1016/j.rineng.2021.100263

[16] Kim, S., Jang, Y., Kim, W., Lee, C., & Park, J. (2025). Dynamic behavior of corrugated cardboard edge damaged by vibration input environments. *Materials*, *18*(18), 4364. https://doi.org/10.3390/ma18184364

[17] Mondal, S., Sahu, S. A., & Goyal, S. (2022). Mathematical analysis of surface wave transference through imperfect interface in FGPM bedded structure. *Mechanics Based Design of Structures and Machines*, *50*(8), 2911–2928. https://doi.org/10.1080/15397734.2020.1790388

[18] Maleki, J., & Jafarzadeh, F. (2023). Model tests on determining the effect of various geometrical aspects on horizontal impedance function of surface footings. *Scientia Iranica*. Advance online publication. https://doi.org/10.24200/sci.2023.59744.6403

[19] Chowdhury, S., Kundu, S., Alam, P., & Gupta, S. (2021). Dispersion of Stoneley waves through the irregular common interface of two hydrostatic stressed MTI media. *Scientia*

Iranica, *28*(2), 837–846. https://doi.org/10.24200/sci.2020.52653.2820

[20] Singh, B., & Kaur, B. (2022). Rayleigh surface wave at an impedance boundary of an incompressible micropolar solid half-space. *Mechanics of Advanced Materials and Structures*, *29*(25), 3942–3949. https://doi.org/10.1080/15376494.2021.1914795

[21] Singh, B., & Kaur, B. (2020). Rayleigh-type surface wave on a rotating orthotropic elastic half-space with impedance boundary conditions. *Journal of Vibration and Control*, *26*(21-22), 1980–1987. https://doi.org/10.1177/1077546320909972

[22] Sahu, S. A., Mondal, S., & Nirwal, S. (2023). Mathematical analysis of Rayleigh waves at the nonplanner boundary between orthotropic and micropolar media. *International Journal of Geomechanics*, *23*(3), 04022313. https://doi.org/10.1061/IJGNAI.GMENG-7246

[23] Giovannini, L. (2022). Theory of dipole-exchange spin-wave propagation in periodically corrugated films. *Physical Review B*, *105*(21), 214426. https://doi.org/10.1103/PhysRevB.105.214426

[24] Rakshit, S., Mistri, K. C., Das, A., & Lakshman, A. (2022). Effect of interfacial imperfections on SH-wave propagation in a porous piezoelectric composite. *Mechanics of Advanced Materials and Structures*, *29*(25), 4008–4018. https://doi.org/10.1080/15376494.2021.1916138

[25] Rakshit, S., Mistri, K. C., Das, A., & Lakshman, A. (2022). Stress analysis on the irregular surface of visco-porous piezoelectric half-space subjected to a moving load. *Journal of Intelligent Material Systems and Structures*, *33*(10), 1244–1270. https://doi.org/10.1177/1045389X211048226

[26] Garbowski, T., & Gajewski, T. (2021). Determination of transverse shear stiffness of sandwich panels with a corrugated core by numerical homogenization. *Materials*, *14*(8), 1976. https://doi.org/10.3390/ma14081976

[27] Ţălu, S. (2015). *Micro and nanoscale characterization of three dimensional surfaces: Basics and applications*. Romania: Napoca Star Publishing House.

[28] Deswal, S., Sheokand, S. K., & Kalkal, K. K. (2019). Reflection at the free surface of fiber-reinforced thermoelastic rotating medium with two-temperature and phase-lag. *Applied Mathematical Modelling*, *65*, 106–119. https://doi.org/10.1016/j.apm.2018.08.004

[29] Anya, A. I., Nwachioma, C., & Ali, H. (2023). Magnetic effects on surface waves in a rotating non-homogeneous half-space with grooved and impedance boundary characteristics. *International Journal of Applied Mechanics and Engineering*, *28*(4), 26–42. https://doi.org/10.59441/ijame/172634

[30] Anya, A. I., & Khan, A. (2019). Propagation and reflection of magneto-elastic plane waves at the free surface of a rotating micropolar fibre-reinforced medium with voids. *Journal of Theoretical and Applied Mechanics*, *57*(4), 869–881. https://doi.org/10.15632/jtam-pl/112066

[31] Othman, M. I., Said, S. M., & Gamal, E. M. (2024). A new model of rotating nonlocal fiber-reinforced visco-thermoelastic solid using a modified Green–Lindsay theory. *Acta Mechanica*, *235*(5), 3167–3180. http://doi.org/10.1007/s00707-024-03874-6

How to Cite: Anya, A. I., & Uche, U. D. (2026). Analysis of Initial Stress and Linearly Variable Amplitudes of Corrugated Surface on a Fibre-Reinforced Solid Under Magnetic Field and Linearly Varying Impedance. *Archives of Advanced Engineering Science*, *4*(3), 247–259. https://doi.org/10.47852/bonviewAAES62027810

Appendix

q11 = A13A15
q12 = (−b2i2A122 − KA13 − b2A132 − (b2 + K)A15)
q13 = (b2 + K)(K + b2A13)